

## BRIGHT COMMON ENVELOPE FORMATION REQUIRES JETS

NOAM SOKER

Department of Physics, Technion, Haifa, 3200003, Israel; soker@physics.technion.ac.il

Version August 28, 2023

### ABSTRACT

I compared with each other and with observations three energy sources to power intermediate luminosity optical transients (ILOTs) and conclude that only jets can power bright ILOTs with rapidly rising lightcurves. I present an expression for the power of the jets that a main sequence secondary star launches as it enters a common envelope evolution (CEE) with a primary giant star. The expression includes the Keplerian orbital period on the surface of the primary star, its total envelope mass, and the ratio of masses. I show that the shock that the secondary star excites in the envelope of the primary star cannot explain bright peaks in the lightcurves of ILOTs, and that powering by jets does much better in accounting for rapidly rising, about 10 days and less, peaks in the lightcurves of ILOTs than the recombination energy of the ejected mass. I strengthen previous claims that jets powered the Great Eruption of Eta Carinae, which was a luminous variable major eruption, and the luminous red novae (LRNe) V838 Mon and V1309 Scorpii. I therefore predict that the ejecta (nebula) of V1309 Scorpii will be observed in a decade or two to be bipolar. My main conclusion is that only jets can power a bright peak with a short rising time of ILOTs (LRNe) at CEE formation.

*Subject headings:* stars: AGB and post-AGB; stars: jets; stars: mass-loss; stars: variables: general; binaries (including multiple): close; planetary nebulae: general

### 1. INTRODUCTION

Intermediate luminosity optical transients (ILOTs) are gravitationally-powered transient events with peak luminosities ranging from somewhat below peak luminosities of classical novae and up to those of typical supernovae (e.g., Mould et al. 1990; Rau et al. 2007; Ofek et al. 2008; Mason et al. 2010; Kasliwal 2011; Tylenda et al. 2011, 2013; Kasliwal 2013; Tylenda et al. 2015; Kamiński et al. 2018; Pastorello et al. 2018; Boian, & Groh 2019; Cai et al. 2019; Jencson et al. 2019; Pastorello et al. 2019; Banerjee et al. 2020; Stritzinger et al. 2020b; Blagorodnova et al. 2021; Pastorello et al. 2021; Bond et al. 2022; Cai et al. 2022a,b; Wadhwa et al. 2022; Karambelkar et al. 2023; Pastorello et al. 2023). The release of gravitational energy can be by mass transfer in a binary system, most likely with the launching of jets by the mass-accreting star (e.g., Kashi et al. 2010; Soker, & Kashi 2016; Kashi 2018; Soker 2020), and/or mass ejection in the equatorial plane (e.g., Pejcha et al. 2017; Hubová & Pejcha 2019). Alternatively, the gravitational energy might result from a merger process of two objects, including the onset of a common envelope evolution (CEE). The later is the focus of this study.

When spatially resolved, the nebulae that ILOTs form are bipolar. The Homunculus nebula that was formed during the Great Eruption of Eta Carinae (e.g., Davidson, & Humphreys 1997) is bipolar. This is a luminous blue variable major eruption which is a type of ILOT. The ILOT V4332 Sgr ejected a bipolar nebula (Kamiński et al. 2018). Most interesting is the ejecta of Nova 1670 (CK Vulpeculae) with its 350-years old bipolar nebula (Shara et al. 1985) because it has an S-morphology

(Kamiński et al. 2020, 2021a). An S-morphology suggests shaping by precessing jets.

I will use the term luminous red novae (LRNe) for those ILOTs that are powered by full merger, but are fainter than typical supernovae. This includes also CEE, whether the companion survives or not the CEE<sup>1</sup>. When a neutron star or a black hole spiral-in inside the envelope of a red supergiant (RSG) star and launch jets the event can be very bright as to mimic a core collapse supernova (CCSN), or even a superluminous CCSN (e.g., Soker, & Gilkis 2018; Gilkis et al. 2019; Grichener & Soker 2019; Yalinewich, & Matzner 2019; Schreier et al. 2021). These events are termed common envelope jets supernovae (CE-JSNe).

LRNe can result from the onset of a CEE with a stellar companion (e.g., Tylenda et al. 2011; Ivanova et al. 2013; Nandez, Ivanova, & Lombardi 2014; Kamiński et al. 2015; Pejcha et al. 2016a,b; Soker 2016a; Blagorodnova et al. 2017; MacLeod et al. 2017, 2018; Segev et al. 2019; Howitt et al. 2020; MacLeod & Loeb 2020; Qian et al. 2020; Schröder et al. 2020; Blagorodnova et al. 2021; Addison et al. 2022; Matsumoto & Metzger 2022; Zhu et al. 2023) or with a sub-stellar (i.e., a brown dwarf or a planet) companion (e.g., Retter & Marom 2003; Retter et al. 2006; Metzger, Giannios, & Spiegel 2012; Yamazaki, Hayasaki, & Loeb 2017; Kashi et al. 2019; Gure-

<sup>1</sup> There is no consensus on these terms (see also Cai et al. 2022b for a review). I refer to all gravitationally-powered transient events as ILOTs (for the usage of the term ILOT see, e.g., Berger et al. 2009; Kashi & Soker 2016; Muthukrishna et al. 2019). Some do not use the ILOT term (e.g., Jencson et al. 2019). There is also no consensus on the set of sub-classes, e.g., Kashi & Soker (2016) versus Pastorello & Fraser (2019) and Pastorello et al. (2019).

vich, Bear, & Soker 2022; De et al. 2023; O’Connor et al. 2023)

Ivanova et al. (2013) study the emission at CEE formation by the recombination of the ionized ejecta (also Howitt et al. 2020). They consider a spherical ejecta, which we now know is not the case with resolves ILOTs because they have bipolar ejecta. This model cannot explain all properties, including the rapid, few days, rise to the second peak (first bright peak) in the light curve of V838Mon and the total energy of the Great Eruption of Eta Carinae. In section 3 I argue that accretion energy that jets deliver is more efficient than recombination energy. Recombination can nicely explain the plateau phase of lightcurves. Matsumoto & Metzger (2022) conduct detailed calculations of the lightcurves due to recombination in CEE. Their results show that the recombination cannot account for a rapidly rising peak and cannot explain some luminous LRNe. For example, in the recombination model of Matsumoto & Metzger (2022) the LRN AT 2014ej requires unreasonable high mass ejection (below I mention that Soker & Kaplan 2021 could fit this LRN with jets).

I studied the role of jets in powering ILOTs in several earlier papers. In Soker (2016a) I studied the energetic of jet-powering in the grazing envelope evolution (GEE). I concluded that during the GEE the jets accelerate the outskirts of the primary envelope to velocities that in some cases bring the flow time to be of the order of the photon diffusion time out of the ejecta,  $t_{\text{flow}} \approx t_{\text{diff,ej}}$ . This implies that a large fraction of the kinetic energy of the jets, which is channelled to thermal energy as the jets collide with the envelope, ends in radiation. This leads to a bright ILOT event. However, in that study I did not examine the luminosity nor did I calculate the accretion rate onto the companion that enters the GEE with the more extended primary star.

In Soker (2020) I demonstrated that the interaction of wide jets with a slower expanding shell is very efficient in channelling the jets’ kinetic energy to radiation. I applied this interaction to three ILOTS: the Great Eruption of Eta Carinae (observational data from, e.g., Davidson, & Humphreys 2012; Rest et al. 2012), to V838 Mon (physical data from Tylenda 2005), and to V4332 Sgr (data from, e.g., Kamiński et al. 2018). I found the jet-shell interaction to be more efficient in converting kinetic energy to radiation than collision of equatorial outflows (e.g., Pejcha et al. 2016a,b). The collision of a fast spherically ejected shell with a slow dense equatorial gas (e.g., Andrews, & Smith 2018; Kurfürst & Krtićka 2019) is more efficient than collision of equatorial ejecta (e.g., Metzger, & Pejcha 2017), but not as that of jet-shell interaction. In any case, fast spherical shell hitting a slower equatorial outflow is not a flow structure that occurs at the formation of CEE. In Soker (2020) I did not deal with the onset of the CEE.

Soker & Kaplan (2021) apply toy models of jet-shell interaction to reproduce the light curves of the ILOTs SNhunt120 (observations by Stritzinger et al. 2020a) and AT 2014ej (an LRN; observations by Stritzinger et al. 2020a). Soker & Kaplan (2021) could fit the light curves with jet-shell interaction (note that the units of times in their two figures should be day). Soker & Kaplan (2021) did not consider the onset of the CEE. These three studies of jet-shell interaction did not examine the accretion

power of the compact object that launches the jets nor did they compare the power with the collision of the companion with the extended envelope.

In the present study I first (section 2) show that the shock that the companion excite in the envelope as it enters a CEE cannot lead to a bright ILOT. In section 3 I compare the luminosity from jets to that from the recombination energy of the ejecta. In section 4 I apply the results to several ILOTs. I summarize in section 5. This study is motivated in part by the recent finding by Mobeen et al. (2023) that the innermost circumstellar material currently surrounding V838 Mon is bipolar.

## 2. POWERING BY JETLESS INTERACTION

In CEE, unlike in supernovae, recombination energy releases energy over a relatively long time, larger than the dynamical time as it requires the envelope to expand, cool, recombines, and for the photons to diffuse out (e.g., Matsumoto & Metzger 2022). Recombination powering cannot explain the rapid rise, less than about 10 days, that is observed in many ILOTs, from luminous blue variables to LRNe (e.g., Cai et al. 2022b for a review).

I schematically present the jetless interaction in the lower panel of Fig. 1. The powering includes recombination energy and the shock that the secondary star excites in the envelope.

A rapid interaction takes place when the secondary star, with mass  $M_2$  and a small radius  $R_2 \ll a$  where  $a$  is the orbital radius, enters the envelope of the primary star, i.e., during the early CEE phase when  $a \simeq R_1$ . I depict this flow structure in the lower panel of Fig. 1. The primary, of mass  $M_1$  and radius  $R_1$ , can be a main sequence and up to a RSG. The secondary excites a shock wave with a typical distance from the orbit which is about the classical Bondi-Hoyle-Lyttleton radius

$$R_{\text{BHL}} = \frac{2GM_2}{c_s^2(a) + v_{\text{rel}}^2(a)} \simeq \frac{2M_2}{M_1}a, \quad (1)$$

where  $v_{\text{rel}} \simeq \sqrt{GM_1/a} - v_{\text{rot}}(a)$ ,  $v_{\text{rot}}(a)$  is the rotation velocity of the envelope at the location of the secondary star, and  $c_s(a)$  is the sound speed. In the second equality I took the denominator to be  $c_s^2(a) + v_{\text{rel}}^2(a) \simeq v_{\text{Kep}}^2(a) = GM_1/a$ . Namely, I assume that the contributions of the sound speed in the envelope and of the envelope rotation more or less cancel each other. To the accuracy of the present study this approximation is adequate.

The Power of the shock, i.e., the rate of channelling kinetic energy to thermal energy, depends on the mass inflow rate into the shock  $\dot{M}_{\text{shock}}$ , its velocity  $v_{\text{shock}}$ , the Mach number, and the shock angle. For an approximate expression in the case of a high mach number shock in the present case I take a perpendicular shock out to radius  $R_{\text{BHL}}$  and  $v_{\text{shock}} \simeq v_{\text{rel}} \simeq \sqrt{GM_1/a}$ , so that  $\dot{M}_{\text{shock}} \simeq \pi R_{\text{BHL}}^2 \rho(a) v_{\text{rel}}$ . This gives for the shock power

$$\begin{aligned} \dot{E}_{\text{shock}} &\simeq \frac{1}{2} \dot{M}_{\text{shock}} v_{\text{shock}}^2 \simeq \frac{\pi}{2} R_{\text{BHL}}^2 v_{\text{rel}}^3 \rho \\ &\simeq 2\pi \left( \frac{M_2}{M_1} \right)^2 (GM_1)^{3/2} a^{1/2} \rho. \end{aligned} \quad (2)$$

The density in the envelope of giant stars varies as  $\rho(r) \propto r^{-\beta}$  with  $\beta \simeq 2 - 3$ . This implies that as the

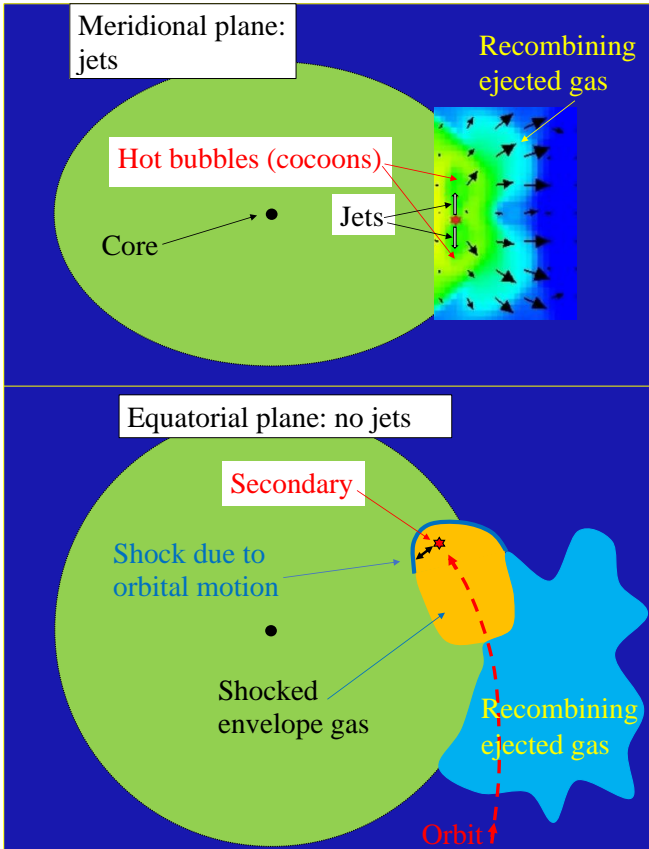


FIG. 1.— A schematic drawing (not to scale) of the three discussed energy sources. Dark blue is a very low-density zone around the binary systems, i.e., the wind of the giant star. The green region is the envelope of the giant star, the small black circle is the core of the giant star, and the red star of David is the secondary star that accretes mass. Upper panel: A schematic drawing in the meridional plane that momentarily contains both the core and the secondary star. The inset with that black arrows is from figure 2 of Schreier, Hillel, & Soker (2023) which is a three-dimensional hydrodynamical simulations of a CEE with jets. The black arrows depict the outflow map. The yellow-coloured zones are higher density than the envelope density (green) that are compressed by the bubble (cocoon) that each of the two jets inflates. Both the shock that the secondary star excite in the envelope (not shown in upper panel) and recombination exist in this case. Lower panel: A schematic drawing in the equatorial plane when the secondary star does not launch jets and shortly after it entered the envelope of the giant star. The dashed-red line depicts the orbit. The double-headed arrow touching the secondary star is about the length of  $R_{\text{BHL}}$ .

secondary spirals-in the power of the shock increases. However, deeper in the envelope the photon diffusion time rapidly increases inward, implying that the fraction of the thermal energy that end in radiation decreases. The expansion time of the post-shock gas inside the accretion radius under the present assumptions, is  $\tau_{\text{exp}} \simeq R_{\text{BHL}}/v_{\text{shock}} \simeq R_{\text{BHL}}/v_{\text{Kep}} \equiv \tau_{\text{f}}$ . The photon diffusion time is  $\tau_{\text{dif},2} \simeq \tau_{\text{R}_{\text{BHL}}}/c$  where  $\tau \simeq \rho\kappa R_{\text{BHL}}$  is the optical depth and  $\kappa$  the opacity. I return to these timescales in section 3.2. I assume that the maximum luminosity is obtained where  $\tau_{\text{exp}} \simeq \tau_{\text{dif},2}$ . This gives for the density at maximum luminosity due to the CEE shock

$$\rho_{\text{max-L}} \simeq \frac{c}{\kappa R_{\text{BHL}} v_{\text{Kep}}}. \quad (3)$$

Substituting this density in equation (2) and assuming that about half of the shock energy ends in radiation, because  $\tau_{\text{dif},2} \simeq \tau_{\text{exp}}$ , yields

$$\begin{aligned} L_{\text{shock}} &\simeq \dot{E}_{\text{shock}}(\rho_{\text{max-L}}) \simeq \frac{\pi}{2} \frac{c}{\kappa} G M_2 \\ &\simeq 1.6 \times 10^4 \left( \frac{\kappa}{0.1 \text{ cm}^2 \text{ g}^{-1}} \right)^{-1} \left( \frac{M_2}{1 M_{\odot}} \right) L_{\odot}. \end{aligned} \quad (4)$$

For scattering on electron opacity the value of  $\kappa$  is larger, implying in turn lower peak luminosity.

As discussed later, the expression (4) gives shock luminosity which is much fainter than most ILOTs.

### 3. JET POWERING

#### 3.1. The power of the jets

In Soker (2016a) I studied the accretion total energy versus the recombination total energy. Here I concentrate on the luminosity. It is useful to express the accretion power at CEE formation in terms of global properties (as masses and orbital period) of the binary system rather than local quantities (i.e., velocity and density). I examine the interaction at CEE formation (onset), i.e.,  $a \simeq R_1$ . I schematically present this flow in the upper panel of Fig. 1. I take the envelope density profile as  $\rho \propto r^{-\beta}$ , where for giant (red giant branch, RGB; asymptotic giant branch, AGB; RSG) stars  $\beta \simeq 2 - 3$ , and so the envelope mass is

$$M_{\text{env}} = \frac{4\pi}{3-\beta} \rho(R_1) R_1^3, \quad \beta < 3. \quad (5)$$

I take the power of the two jets that the secondary star launches to be  $\dot{E}_{2j} = \eta_{2j} \dot{E}_{\text{acc}}$ , where the BHL accretion power is  $E_{\text{acc}} = G M_2 M_{\text{BHL}} / 2 R_2$ . Using the same assumptions as in section 2, i.e., equation (1), gives for  $a \simeq R_1$

$$\begin{aligned} \dot{E}_{2j}(R_1) &\simeq \eta_{2j} \pi \frac{G M_2}{2 R_2} R_{\text{BHL}}^2 \rho(R_1) v_{\text{rel}}(R_1) \\ &\simeq \left( \frac{M_2}{M_1} \right)^2 \eta_{2j} \pi (3 - \beta) \frac{G M_2 M_{\text{env}}}{R_2 \tau_{\text{Kep}}}, \end{aligned} \quad (6)$$

where  $\tau_{\text{Kep}} = 2\pi R_1^{3/2} / (G M_1)^{1/2}$  is the Keplerian orbital period on the surface of the primary star and where quantities are calculated near the primary surface, i.e., when  $a \simeq R_1$ .

I scale equation (6) for a main sequence companion to yield

$$\begin{aligned} \dot{E}_{2j}(R_1) &\simeq 10^5 (3 - \beta) \left( \frac{\eta_{2j}}{0.1} \right) \left( \frac{M_2/R_2}{M_{\odot}/R_{\odot}} \right) \\ &\times \left( \frac{M_2}{0.1 M_1} \right)^2 \left( \frac{M_{\text{env}}}{1 M_{\odot}} \right) \left( \frac{\tau_{\text{Kep}}}{1 \text{ yr}} \right)^{-1} L_{\odot}. \end{aligned} \quad (7)$$

In the derivation here the parameter  $\eta_{2j}$  includes both the reduction in the actual accretion rate relative to the BHL accretion rate, and the fraction of energy carried by the jets relative to the actual accretion energy (see also section 3.2).

If a fully ionized solar-composition gas is ejected from the envelope and recombines on a rate of  $\dot{M}_{\text{ej,rec}}$  as it

leaves the star and cools, the power the recombination releases is

$$\dot{E}_{\text{rec}} = 2.5 \times 10^5 \left( \frac{\dot{M}_{\text{ej,rec}}}{1M_{\odot} \text{ yr}^{-1}} \right) L_{\odot}. \quad (8)$$

This is actually an upper limit on the radiation due to recombination because a fraction of this energy might end in unbinding envelope gas and accelerating it out.

Numerical simulations of CEE that do not include extra energy source of recombination (which here is assumed to end in radiation) and jets show that the ejection of the envelope proceeds on a longer time than the Keplerian orbital period on the surface of the star (as I discuss in section 4.4). A timescale that is not much longer than several times the Keplerian period on the surface of the primary requires a secondary of mass  $M_2 > 0.1M_1$ . The timescale over which the recombination power is released is longer than the ejection time itself, i.e., the time to unbind the gas, because the gas needs to expand and cool for it to recombine. From equations (7) and (8) I scale therefore the power ratio of the two energy sources to be

$$\frac{\dot{E}_{2j}(R_1)}{\dot{E}_{\text{rec}}} \simeq 4(3 - \beta) \left( \frac{\eta_{2j}}{0.1} \right) \left( \frac{M_2/R_2}{M_{\odot}/R_{\odot}} \right) \times \left( \frac{M_2}{0.1M_1} \right)^2 \left( \frac{\dot{M}_{\text{ej,rec}}}{0.1M_{\text{env}}\tau_{\text{Kep}}^{-1}} \right)^{-1}. \quad (9)$$

I note here that the relevant time for  $\dot{M}_{\text{ej,rec}}$  is not the ejection time itself, but rather the time it takes the ejected gas to recombine.

The critical question is then the fraction of the jets' energy that ends in radiation. Here jets have another advantage over recombination energy. Jets can propagate and deposit most of their energy in the outer regions of the ejecta where the photon diffusion time out is shorter; see Kaplan & Soker (2020) and Soker (2020) for the interaction of jets with a shell and the radiation fraction. This might be significant as dust might substantially increase opacity in these transients (e.g., González-Bolívar et al. 2023).

### 3.2. Time scales

The accretion power might exceed the Eddington limit. However, I note that the process of radiation diffusion does not reach a steady state. To show that I consider four timescales.

I define the flow timescale to be the time during which the secondary star crosses the accretion radius under the present assumptions. This is about the time for a mass element to reach the accreting body after it crosses the accretion radius. Substituting the relevant variables and scaling under the present assumptions gives

$$\tau_{\text{f}} \equiv \frac{R_{\text{BHL}}}{v_{\text{Kep}}} = 0.03 \left( \frac{M_2}{0.1M_1} \right) \left( \frac{\tau_{\text{Kep}}}{1 \text{ yr}} \right) \text{ yr}. \quad (10)$$

I also define the accretion timescale for the accretion disk around the secondary star, namely the viscous timescale of the accretion disk. This timescale is  $\approx 100$  times the Keplerian period of the disk size. Taking the disk radius to be of the order of the secondary radius, which is adequate for a main sequence companion in a CEE, this

timescale is crudely given by

$$\tau_{\text{vis}} \approx 100 \frac{2\pi R_2^{3/2}}{\sqrt{GM_2}} = 0.03 \times \left( \frac{M_2}{1M_{\odot}} \right)^{-1/2} \left( \frac{R_2}{1R_{\odot}} \right)^{3/2} \text{ yr}. \quad (11)$$

Consider then that the accreted mass releases energy near the surface of the secondary star. A large fraction of this energy, and even most of it, is carried by the jets on a timescale,  $\tau_{j,2} \simeq k_j R_{\text{BHL}}/v_j$ , where  $v_j$  is the velocity of the jets and with the parameter  $k_j > 1$  I take into account that a jet slows down as it interacts with the envelope. To power a bright transient event the jets should reach close to the surface of the envelope, and so I assume that the jets do not slow down much from their terminal velocity, which is about the escape velocity from the secondary star. I scale with  $k_j = 2$ . With the aid of equation (1) and  $a \simeq R_1$ , as the secondary is in the outer regions of the envelope, this reads for a main sequence secondary star

$$\tau_{j,2} \simeq \frac{R_{\text{BHL}}}{v_j} \simeq 0.0035 \left( \frac{k_j}{2} \right) \left( \frac{M_2}{0.1M_1} \right) \times \left( \frac{R_1}{200R_{\odot}} \right) \left( \frac{v_j}{500 \text{ km s}^{-1}} \right)^{-1} \text{ yr}. \quad (12)$$

For the photon diffusion time I take the density of the accreted gas inside  $R_{\text{BHL}}$  to be as that in the envelope by equation (5). The optical depth is then  $\simeq R_{\text{BHL}}\rho(R_1)\kappa$ , where  $\kappa$  is the opacity. The density is actually somewhat higher, increasing further the diffusion time. Under the present assumptions the diffusion time is

$$\tau_{\text{dif},2} \simeq \frac{R_{\text{BHL}}}{c} R_{\text{BHL}}\rho(R_1)\kappa \simeq 0.2(3 - \beta) \left( \frac{\kappa}{0.4 \text{ cm}^2 \text{ g}^{-1}} \right) \times \left( \frac{M_2}{0.1M_1} \right)^2 \left( \frac{R_1}{200R_{\odot}} \right)^{-1} \left( \frac{M_{\text{env}}}{1M_{\odot}} \right) \text{ yr}. \quad (13)$$

From the above four timescales we learn the following. The removal of energy by the jets is fast. It can bring the accretion processes to a semi-steady state (not a full steady state because the secondary star spirals-in). On the other hand, the photon diffusion time is longer than all timescales. This means that if indeed the secondary star launches jets, as I assume here, then jets carry most of the accretion energy. In that respect the Eddington limit is less relevant in reducing the accretion rate. Namely, the removal of energy by the jets makes the power carried by radiation to be sub-Eddington. The energy that the jets carry do indeed reduce the accretion rate in what is termed the negative jet feedback mechanism (for a review see Soker 2016b), as was shown numerically by Grichener, Cohen, & Soker (2021) in one-dimension and by Hillel, Schreier, & Soker (2022) in three dimensions. This reduction in the accretion rate in this study enters the parameter  $\eta_{2j}$ . At the peak of the accretion process the power of the jets might be up to  $\approx 10^2 - 10^3$  times the Eddington luminosity limit. This is possible for two reasons. The first is that the jets counteract accretion only along the polar directions. Indeed, no accretion occurs along the polar directions. However, accretion proceeds from the equatorial plane vicinity. The

second one is that, as stated above, eventually the jets do reduce the accretion rate by depositing energy to the envelope from which accretion takes place. Namely, the highly-super-Eddington phase is temporarily one.

#### 4. IMPLICATIONS TO SPECIFIC SYSTEMS

##### 4.1. *The Great Eruption of Eta Carinae*

The second peak of the Great Eruption of Eta Carinae had a rapid rise by as much as  $\Delta L > 10^7 L_\odot$  that lasted few days. By equation (4) a passage of the secondary inside the envelope of the primary would require the opacity to be as low as  $\kappa \simeq 0.01 \text{ cm}^2 \text{ g}^{-1}$  for a secondary star of  $M_2 = 100 M_\odot$ . This is a too low opacity and a too massive secondary star for this system. Clearly a shock excited by the secondary star as it orbits through the primary stellar envelope cannot explain the Great Eruption.

The mass loss rate in the 20 years duration of the great eruption was  $\simeq 1 M_\odot \text{ yr}^{-1}$  (e.g., [Smith 2008](#)). The companion is a massive star so that  $M_2 \simeq 0.3 M_1$ . The fast wind from the companion of  $\simeq 3000 \text{ km s}^{-1}$  suggests that  $M_2/R_2 \gtrsim 4 M_\odot/R_\odot$ . The Keplerian period on the surface of the primary, assuming that it was the size of the periastron passage at the Great eruption, in this eccentric  $e \simeq 0.9$  orbit of 5.54 yr is  $\simeq 0.2 \text{ yr}$ . However, I consider global properties and take here  $\tau_{\text{Kep}} = 5.5 \text{ yr}$  during the Great Eruption ([Damineli 1996](#)). For the envelope mass of the primary star I take  $100 M_\odot$ . Equation (7) gives for the above quantities  $\dot{E}_{2j} \approx 6 \times 10^7 L_\odot$ . This energy can account for the peak luminosity of  $\simeq 10^7 L_\odot$  if a fraction of  $\eta_{\text{rad},2j} \simeq 0.2$  of the jets' energy is channelled to radiation.

For the same quantities equation (9) gives  $\dot{E}_{2j}(R_1)/\dot{E}_{\text{rec}} \approx 70$ . This implies that the jets have much larger power than the recombination energy. [Ivanova et al. \(2013\)](#) found already that recombination energy cannot account for the Great Eruption of Eta Carinae.

As the bipolar structure of the Homunculus suggests, the Great Eruption of Eta Carinae was powered by jets (e.g., [Soker 2001](#); [Kashi & Soker 2010](#)). This is true whether the system did not enter a full CEE as in the binary interaction scenario for the Great Eruption, which already includes jets (e.g., [Soker 2001, 2007](#)), or whether a binary system entered a CEE in the triple star scenario for the Great Eruption (e.g., [Livio & Pringle 1998](#); [Portegies Zwart & van den Heuvel 2016](#); [Hirai et al. 2021](#))<sup>2</sup>. In the binary model the secondary star grazed the primary stellar envelope during periastron passages and accreted mass via an accretion disk that launched the jets (e.g., [Kashi & Soker 2010](#)).

##### 4.2. *V838 Mon*

<sup>2</sup> These studies of triple system progenitor of the Great Eruption ignore jets. In any case, I find that the triple-star scenario of a merger in an unstable triple system ([Portegies Zwart & van den Heuvel 2016](#); [Hirai et al. 2021](#)) has problems. (i) There was a second outburst in 1890-1895 (the Lesser Eruption; [Humphreys, Davidson, & Smith 1999](#)) that according to this scenario requires another merger. (ii) The present binary system shares an equatorial plane with the Homunculus nebula (e.g., [Madura et al. 2012](#)). This is hard to explain in a non-coplanar triple system as the merger scenarios require. (iii) The scenario of [Hirai et al. \(2021\)](#) requires the presence of a dense equatorial gas that is not observed in the Homunculus.

The light curve of V838 Mon shows several peaks. A weak outburst followed by three peaks of  $L \simeq 10^6 L_\odot$  ([Munari et al. 2002](#)). The rise to the first bright peak of V838 Mon lasted for about 4 days and reached  $L_{\text{peak}} = 1.2 \times 10^6 L_\odot$  ([Tylenda 2005](#)). For a shock excited by a companion to explain this peak the secondary mass according to equation (4) should be  $> 10 M_\odot$  even if the opacity is reduced to  $\kappa = 0.01 \text{ cm}^2 \text{ g}^{-1}$ . However, the primary itself is  $M_1 < 8 M_\odot$ , and so I conclude that shock in a CEE cannot explain the bright peaks in the lightcurve of V838 Mon.

Consider next recombination energy. [Matsumoto & Metzger \(2022\)](#) fit the plateau phase of V838 Mon with an ejecta mass of  $M_{\text{ej}} \simeq 4.2 M_\odot$  and an average velocity of  $860 \text{ km s}^{-1}$ . The problems with this fitting is that the ejected mass is too large for a main sequence star of mass  $M_1 < 8 M_\odot$  and the required velocity is larger than the observed one (e.g., [Munari et al. 2002](#); [Blagorodnova et al. 2021](#)). In any case, their fitting by recombination energy does not aim to explain the 4 days rise of the first bright peak. They assume that it resulted from cooling of the hot ejected mass. However, in a time of 4 days (the rise time of the first bright peak) gas with a velocity of  $860 \text{ km s}^{-1}$  expands to a distance of  $r \simeq 3 \times 10^{13} \text{ cm}$ . The optical depth is  $\tau \simeq \kappa M_{\text{ej}}/4\pi r^2 = 7.5 \times 10^4 (\kappa/0.1 \text{ cm}^2 \text{ g}^{-1})$ . It is unlikely that at such a high optical depth the ejecta will form the rapid rise by radiative cooling.

I keep the scaling of equation (9) beside the last term. The effective mass ejection rate for recombination should be the mass divided by the plateau, which for V838 Mon is about 70 days. Taking  $M_{\text{ej}} \simeq 4.2 M_\odot$  as above and the Keplerian time of the B-type progenitor to be  $< 0.5 \text{ day}$  (depending on the radius at outburst) and  $M_{\text{env}} \simeq 1 M_\odot$ , I find from equation (9)  $\dot{E}_{2j}(R_1)/\dot{E}_{\text{rec}} \approx 100$ . For these quantities equation (7) gives (with the other parameters as in the scaling)  $\dot{E}_{2j} \approx 10^8 L_\odot$ , implying that the jets can account for the kinetic energy of the ejecta and the radiation.

Before concluding I note that the outburst of V838 Mon could have resulted from the disruption of a low-mass pre-main sequence star on the primary star rather than the onset of a CEE ([Soker & Tylenda 2003](#); [Tylenda & Soker 2006](#)). I still claim it was powered by jets, but in that case jets that the primary star launched as it accreted the disrupted secondary mass via an accretion disk.

I conclude that V838 Mon was most likely powered by jets, in particular the first bright peak. Indeed, the bipolar structure of its inner ejecta that was established recently by [Mobeen et al. \(2023\)](#) (for earlier hints see [Chesneau et al. 2014](#); [Kamiński et al. 2021](#); [Mobeen et al. 2021](#)) and the point-symmetry of the clumps they find strongly suggests that jets were the main powering source of this ILOT. The shock that the companion excites in the primary envelope and recombination energy add some small fraction to the powering and radiation.

##### 4.3. *V1309 Scorpii*

V1309 Scorpii had a roughly exponential rise in brightness during outburst, rising by a factor of about 100 in the last 10 days to  $L = 3 \times 10^4 L_\odot$  ([Tylenda et al. 2011](#)). [Nandez, Ivanova, & Lombardi \(2014\)](#) build

a model for V1309 where the primary and secondary masses are  $M_1 = 1.52M_\odot$  and  $M_2 = 0.16M_\odot$ , respectively. Unless the companion is more massive and opacity much lower than  $0.1 \text{ cm}^2 \text{ g}^{-1}$ , I find from equation (4) that shock at CEE formation cannot explain the peak of this outburst.

I examine powering by recombination. The lightcurve of V1309 Scorpii has a faint peak (e.g., compared with V838 Mon), and the rise to the maximum is exponential rather than with a steep step. Matsumoto & Metzger (2022) fit the peak with an ejecta mass of  $M_{\text{ej}} \simeq 0.032M_\odot$  and an average velocity of  $550 \text{ km s}^{-1}$ . Although the ejected mass is easily accommodate by a progenitor of  $M_1 \simeq 1M_\odot$ , the required velocity is much larger than the observed velocity of the ejecta of V1309 Scorpii which is  $\simeq 150 \text{ km s}^{-1}$  (Tylenda et al. 2011; Blagorodnova et al. 2021). Another problem is that the light curve that results from recombination energy as Matsumoto & Metzger (2022) calculate has a rise time about equal to decline time. In V1309 Scorpii the rise time is much shorter than the decline time (Tylenda et al. 2011).

With a primary envelope mass of  $M_{\text{env}} = 1M_\odot$ , a Keplerian time of  $\tau_{\text{Kep}} = 0.1 \text{ day}$ , ejected mass of  $M_{\text{ej}} = 0.032M_\odot$  as above, and a plateau time of  $\simeq 20 \text{ days}$ , which is the relevant time for the recombination timescale and which gives  $M_{\text{ej,rec}} \simeq 0.6M_\odot \text{ yr}^{-1}$ , I find from equation (9) that  $\dot{E}_{2j}(R_1)/\dot{E}_{\text{rec}} \approx 2000$ . Clearly accretion power at the peak can dominate the recombination power.

It seems that V1309 Scorpii was also powered by jets with a lesser contribution from recombination. I predict that its ejecta has a bipolar morphology. Observations in about a decade or two might resolve the structure of the ejecta (for a distance of 3 kpc and an expansion velocity of  $150 \text{ km s}^{-1}$ ; Tylenda et al. 2011).

#### 4.4. Progenitors of planetary nebulae

I consider the onset of CEE of RGB and AGB stars with main sequence secondary stars, i.e., progenitor systems of planetary nebulae. Soker & Kashi (2012) suggested that some bipolar PNe formation involve one or more ILOT events. They could only estimate the luminosity of these speculated ILOTs, and give the range of  $L_{\text{PN,ILOT}} \simeq 3 \times 10^4 L_\odot - 10^7 L_\odot$ . More reasonable range would be  $L_{\text{PN,ILOT}} \simeq 10^5 L_\odot - 10^6 L_\odot$ . The formation of a bright ILOT during mass ejection of a bipolar PN requires a relatively massive secondary star, i.e.,  $M_2 \gtrsim 0.5M_\odot$  and that its jets shape the large lobes.

Simulations show that without the inclusion of the recombination energy of the unbound gas the mass ejection rate during CEE of RGB, AGB and RSG stars is  $< M_{\text{env}}/\tau_{\text{Kep}}$  (e.g., Nandez & Ivanova 2016; Kramer et al. 2020; Reichardt et al. 2020; Sand et al. 2020; Glanz & Perets 2021; González-Bolívar et al. 2022; Lau et al. 2022; see Roepke & De Marco 2023 for a review). High mass ejection rates of  $\approx M_{\text{env}}/\tau_{\text{Kep}}$  can also be achieved without recombination energy if the secondary star is massive,  $M_2 \gtrsim 0.5M_1$ , (e.g., Ricker & Taam 2012).

Sand et al. (2020) conduct CEE simulations with an AGB primary star. They find that the mass ejection rates can reach values close to  $M_{\text{env}}/\tau_{\text{Kep}}$  only when the

recombination energy is channelled to mass ejection<sup>3</sup>. In that case of course the recombination energy does not contribute much to the lightcurve of the event.

Overall, when most of the recombination energy goes to radiation, the scaling of equation (9) is appropriate for binary progenitors of planetary nebulae. For a more massive secondary star with  $M_2 > 0.1M_1$  the mass ejection rate might be larger, but the inequality  $\dot{E}_{2j}(R_1) > \dot{E}_{\text{rec}}$ , or even  $\dot{E}_{2j}(R_1) \gg \dot{E}_{\text{rec}}$ , hold. Again, photon diffusion time out from the interaction zone of the jets with the shell (ejecta),  $t_{\text{diff,ej}}$ , is expected to be shorter than the recombination timescale, making the rise time shorter for jets' powering than for recombination. Overall, I conclude that bright peaks with short rise time during CEE formation of planetary nebula progenitors are likely to be powered by jets.

As for the peak luminosity itself at CEE formation, the scaling of equation (7) is appropriate, but for bipolar planetary nebulae with a main sequence companion I would expect  $M_2 \gtrsim 0.3M_1$ . Not all the jets' energy ends in radiation, but when the companion is in the outer zone of the envelope, a large fraction  $\eta_{\text{rad},2j}$  might end in radiation. Overall, I scale the jet-powered peak radiation at CEE formation of planetary nebula progenitors by the crude estimate

$$L_{\text{CE,PN}} \simeq 3 \times 10^5 (3 - \beta) \left( \frac{\eta_{\text{rad},2j}}{0.3} \right) \left( \frac{\eta_{2j}}{0.1} \right) \times \left( \frac{M_2}{0.3M_1} \right)^2 \left( \frac{M_2/R_2}{M_\odot/R_\odot} \right) \left( \frac{M_{\text{env}}}{1M_\odot} \right) \left( \frac{\tau_{\text{Kep}}}{1 \text{ yr}} \right)^{-1} L_\odot \quad (14)$$

This is much brighter than the emission due the shock that the orbital motion of the companion excites in the envelope (equation 4).

The peak in the light curve that the jets power might last for a time much shorter than the Keplerian time. The emission at later times after the companion plunge into the envelope will come from both jets and recombination energy, or only from recombination energy. The peak emission at this phase will be longer and fainter than the peak at CEE formation.

I summarize the relevant properties of the three ILOTs and the CEE formation by planetary nebula progenitors in Table 1.

## 5. SUMMARY

I compared with each other and with observations three energy sources to power ILOTs (LRNe) at CEE formation (including GEE formation). I presented the power of the energy sources in terms of global properties of the binary system for the shock that the secondary star excites in the envelope of the primary star (equation 4), for the power of the jets that the secondary star launches (equation 7), and for the recombination energy (equation 8). Equation (9) gives the ratio of jets' power to recombination power. In comparing to the properties of emission powered by the recombination energy I used also the results of Ivanova et al. (2013) and Matsumoto & Metzger (2022).

I compared these energy sources with three observed ILOTs, the Great Eruption of Eta Carinae in section 4.1,

<sup>3</sup> I do not refer to the very early mass ejection rates that their graphs show at the beginning of the simulations as these seem numerical adjustments.

TABLE 1  
BINARY PROPERTIES OF STUDEID ILOTS

Object	$M_1$ $M_\odot$	$M_2$ $M_\odot$	$\dot{M}_{\text{ej,rec}}$ $M_\odot \text{ yr}^{-1}$	$M_{\text{env}}$ $M_\odot$	$\tau_{\text{Kep}}$ year	$\dot{E}_{2j}$ $L_\odot$	$\dot{E}_{2j}/\dot{E}_{\text{rec}}$
GE Eta Car	$\simeq 120 - 200$	$\simeq 30 - 90$	$\simeq 1$	$= 100$	$= 5.5$	$\approx 10^8$	$\approx 70$
V838 Mon	$= 6$	$\simeq 0.5$	$\approx 10$	$\simeq 1$	$\simeq 10^{-3}$	$\approx 10^8$	$\approx 100$
V1309 Scorpii	$= 1.5$	$\simeq 0.15$	$\approx 0.6$	$\simeq 1$	$3 \times 10^{-4}$	$\approx 10^8$	$\approx 2000$
CEE-PNe	$= 1 - 5$	$\simeq 0.3 - 1$	$[\approx 0.1]^*$	$\simeq 1$	$\simeq 1$	$\approx 40$	$[\approx 10^6]^*$

The binary properties (columns 2-6) that I use in this study to calculate the jets' power (next to last column by equation 7) and its ratio to the recombination power (last column by equation 9). The input parameters from left to right are the name of the system, the primary stellar mass, the secondary stellar mass, the recombination rate of the ejected gas if recombination powers the plateau of the lightcurve, the envelope mass of the primary star, and the Keplerian period on the surface of the primary star. The sources to the different values are from papers cited in the text. The input parameters of the different systems can be within uncertainties of up to few tens of percent ( $=$ ), up to a factor of a few ( $\simeq$ ), or up to about an order of magnitude ( $\approx$ ). The derived quantities are uncertain by about an order of magnitude. Abbreviation: CEE-PNe: CEE formation by planetary nebula progenitors; GE Eta Car: The Great Eruption of Eta Carinae.  $\star$  In the case of CEE formation by planetary nebula progenitors there are no direct observations of any ILOT with an estimated ejecta recombination rate. I therefore take  $\dot{M}_{\text{ej,rec}} \approx 0.1M_\odot \text{ yr}^{-1}$  as a demonstrative example.

with V838 Mon in section 4.2, and with V1309 Scorpii in section 4.3. In all three cases the shock that the secondary star excites in the envelope falls short of explaining the peak luminosity in the lightcurve. In all three cases recombination powering yields a rise time to peak luminosity that is too long to explain the observed rapid rise to the first bright peak. In contrast, I find that the energy that the jets can supply explains the rapid rise and peak luminosity in all three ILOTs. I predict that the ejecta (nebula) of V1309 Scorpii will be observed in a decade or two to be bipolar. I summarised the relevant properties in table 1.

Although the claim for jet-powering of these ILOTs have been made in the past (see section 4), this study for the first time systematically compares the three energy sources with each other and with these ILOTs. This study also presents the jets' power by the global properties of the primary star, i.e., the Keplerian period on the surface of the primary star and its total envelope mass (rather than the local properties of density and velocity). Most of all, this study aims at the CEE formation phase.

In section 4.4 I applied the results to CEE (or GEE) formation phase during the ejection of planetary nebulae. I presented the scaled equation (14) for the expected peak luminosity when a main sequence companion enters the envelope of an RGB star or an AGB star. This peak luminosity is compatible with the range of estimated luminosities of the ILOTs that Soker & Kashi (2012) speculated to have occurred at the formation of four bipolar planetary nebulae. I concluded that only jets can power bright ILOTs (LRNe) at CEE formation.

This study adds to the accumulating evidences, observationally and theoretically, that jets serve as the main powering source of most ILOTs (including LRNe and luminous blue variable major eruptions).

#### ACKNOWLEDGEMENTS

I thank Amit Kashi and an anonymous referee for useful comments. This research was supported by a grant from the Pazy Research Foundation.

#### REFERENCES

- Addison H., Blagorodnova N., Groot P. J., Erasmus N., Jones D., Mogawana O., 2022, MNRAS, 517, 1884.  
 Andrews, J. E., & Smith, N. 2018, MNRAS, 477, 74  
 Banerjee, D. P. K., Geballe, T. R., Evans, A., Shahbandeh, M., Woodward, C. E., Gehrz, R. D., Eyres, S. P. S., Starrfield, S. & Zijlstra, A. 2020, ApJ, 904, L23.  
 Berger, E., Soderberg, A. M., Chevalier, R. A., et al. 2009, ApJ, 699, 1850  
 Blagorodnova, N., Klencki, J., Pejcha, O., Vreeswijk, P. M., Bond, H. E., Burdge, K. B., De, K., et al. 2021, A&A, 653, A134.  
 Blagorodnova, N., Kotak, R., Polshaw, J., et al. 2017, ApJ, 834, 107  
 Boian, I., & Groh, J. H. 2019, A&A, 621, A109.  
 Bond H. E., Jencson J. E., Whitelock P. A., Adams S. M., Bally J., Cody A. M., Gehrz R. D., et al., 2022, ApJ, 928, 158.  
 Cai Y.-Z., Pastorello A., Fraser M., Wang X.-F., Filippenko A. V., Reguitti A., Patra K. C., et al., 2022a, A&A, 667, A4.  
 Cai, Y.-Z., Pastorello, A., Fraser, M., et al. 2019, A&A, 632, L6  
 Cai Y., Reguitti A., Valerin G., Wang X., 2022b, Univ, 8, 493.  
 Chesneau O., Millour F., De Marco O., Bright S. N., Spang A., Banerjee D. P. K., Ashok N. M., et al., 2014, A&A, 569, L3.  
 Damiani A., 1996, ApJL, 460, L49.  
 Davidson, K., & Humphreys, R. M. 1997, ARA&A, 35, 1  
 Davidson, K., & Humphreys, R. M. 2012, Nature, 486, E1  
 De K., MacLeod M., Karambelkar V., Jencson J. E., Chakrabarty D., Conroy C., Dekany R., et al., 2023, Natur, 617, 55.  
 Gilkis, A., Soker, N., & Kashi, A. 2019, MNRAS, 482, 4233  
 Glanz H., Perets H. B., 2021, MNRAS, 507, 2659.  
 González-Bolívar M., Bermúdez-Bustamante L. C., De Marco O., Siess L., Price D. J., Kasliwal M., 2023, arXiv:2306.16609  
 González-Bolívar M., De Marco O., Lau M. Y. M., Hirai R., Price D. J., 2022, MNRAS, 517, 3181.  
 Grichener A., Cohen C., Soker N., 2021, ApJ, 922, 61.  
 Grichener A., Soker N., 2019, ApJ, 878, 24.  
 Gurevich O., Bear E., Soker N., 2022, MNRAS, 511, 1330.  
 Hillel S., Schreier R., Soker N., 2022, MNRAS, 514, 3212.  
 Hirai R., Podsiadlowski P., Owocki S. P., Schneider F. R. N., Smith N., 2021, MNRAS, 503, 4276.  
 Howitt, G., Stevenson, S., Vigna-Gómez, A., Justham, S., Ivanova, N., Woods, T. E., Neijssel, C. J., & Mandel, I. 2020, MNRAS, 492, 3229.  
 Hubová D., Pejcha O., 2019, MNRAS, 489, 891.  
 Humphreys R. M., Davidson K., Smith N., 1999, PASP, 111, 1124.  
 Ivanova N., 2017, IAUS, 329, 199.  
 Ivanova, N., Justham, S., Avendano Nandez, J. L., & Lombardi, J. C. 2013, Science, 339, 433  
 Jencson, J. E., Kasliwal, M. M., Adams, S. M., et al. 2019, ApJ, 886, 40

- Kamiński T., Mason E., Tylanda R., Schmidt M. R., 2015, *A&A*, 580, A34.
- Kamiński T., Menten K. M., Tylanda R., Wong K. T., Belloche A., Mehner A., Schmidt M. R., et al., 2020, *A&A*, 644, A59.
- Kamiński T., Steffen W., Bujarrabal V., Tylanda R., Menten K. M., Hajduk M., 2021a, *A&A*, 646, A1.
- Kamiński T., Steffen W., Tylanda R., Young K. H., Patel N. A., Menten K. M., 2018, *A&A*, 617, A129.
- Kamiński T., Tylanda R., Kiljan A., Schmidt M., Lisiecki K., Melis C., Frankowski A., et al., 2021, *A&A*, 655, A32.
- Kaplan N., Soker N., 2020, *MNRAS*, 492, 3013.
- Karambelkar V. R., Kasliwal M. M., Blagorodnova N., Sollerman J., Aloisi R., Anand S. G., Andreoni I., et al., 2023, *ApJ*, 948, 137.
- Kashi, A. 2018, *Galaxies*, 6, 82.
- Kashi, A., Frankowski, A., & Soker, N. 2010, *ApJ*, 709, L11
- Kashi, A., Michaelis, A. M., & Feigin, L. 2019, *Galaxies*, 8, 2.
- Kashi A., Soker N., 2010, *ApJ*, 723, 602.
- Kashi, A., & Soker, N. 2016, *Research in Astronomy and Astrophysics*, 16, 99
- Kasliwal, M. M. 2011, *Bulletin of the Astronomical Society of India*, 39, 375
- Kasliwal, M. M. 2013, *IAU Symposium*, 281, 9
- Kramer M., Schneider F. R. N., Ohlmann S. T., Geier S., Schaffenroth V., Pakmor R., Röpke F. K., 2020, *A&A*, 642, A97.
- Kurfürst, P., & Krtićka, J. 2019, *A&A*, 625, A24
- Lau M. Y. M., Hirai R., González-Bolívar M., Price D. J., De Marco O., Mandel I., 2022, *MNRAS*, 512, 5462.
- Livio M., Pringle J. E., 1998, *MNRAS*, 295, L59.
- MacLeod, M. & Loeb, A. 2020, *ApJ*, 895, 29.
- MacLeod, M., Macias, P., Ramirez-Ruiz, E., Grindlay, J., Batta, A., & Montes, G. 2017, *ApJ*, 835, 282
- MacLeod, M., Ostriker, E. C., & Stone, J. M. 2018, *ApJ*, 868, 136.
- Madura T. I., Gull T. R., Owocki S. P., Groh J. H., Okazaki A. T., Russell C. M. P., 2012, *MNRAS*, 420, 2064.
- Mason, E., Diaz, M., Williams, R. E., Preston, G., & Bensby, T. 2010, *A&A*, 516, A108
- Matsumoto T., Metzger B. D., 2022, *ApJ*, 938, 5.
- Metzger B. D., Giannios D., Spiegel D. S., 2012, *MNRAS*, 425, 2778.
- Metzger, B. D., & Pejcha, O. 2017, *MNRAS*, 471, 3200
- Mobeen M. Z., Kamiński T., Matter A., Wittkowski M., et al., 2023,
- Mobeen M. Z., Kamiński T., Matter A., Wittkowski M., Paladini C., 2021, *A&A*, 655, A100.
- Mould, J., Cohen, J., Graham, J. R., et al. 1990, *ApJ*, 353, L35
- Munari U., Henden A., Kiyota S., Laney D., Marang F., Zwitter T., Corradi R. L. M., et al., 2002, *A&A*, 389, L51.
- Muthukrishna, D., Narayan, G., Mandel, K. S., Biswas, R., & Hložek, R. 2019, *PASP*, 131, 118002
- Nandez J. L. A., Ivanova N., 2016, *MNRAS*, 460, 3992.
- Nandez J. L. A., Ivanova N., Lombardi J. C., 2014, *ApJ*, 786, 39.
- O'Connor C. E., Bildsten L., Cantiello M., Lai D., 2023, *ApJ*, 950, 128. doi:10.3847/1538-4357/acd2d4
- Ofek, E. O., Kulkarni, S. R., Rau, A., et al. 2008, *ApJ*, 674, 447
- Pastorello, A., & Fraser, M. 2019, *Nature Astronomy*, 3, 676
- Pastorello, A., Kochanek, C. S., Fraser, M., et al. 2018, *MNRAS*, 474, 197
- Pastorello, A., Mason, E., Taubenberger, S., et al. 2019, *A&A*, 630, A75
- Pastorello, A., Valerin, G., Fraser, M., Elias-Rosa, N., Valenti, S., Reguitti, A., Mazzali, P. A., et al. 2021, *A&A*, 647, A93.
- Pastorello A., Valerin G., Fraser M., Reguitti A., Elias-Rosa N., Filippenko A. V., Rojas-Bravo C., et al., 2023, *A&A*, 671, A158.
- Pejcha, O., Metzger, B. D., & Tomida, K. 2016a, *MNRAS*, 455, 4351
- Pejcha, O., Metzger, B. D., & Tomida, K. 2016b, *MNRAS*, 461, 2527
- Pejcha O., Metzger B. D., Tyles J. G., Tomida K., 2017, *ApJ*, 850, 59.
- Portegies Zwart S. F., van den Heuvel E. P. J., 2016, *MNRAS*, 456, 3401.
- Qian S.-B., Zhu L.-Y., Liu L., Zhang X.-D., Shi X.-D., He J.-J., Zhang J., 2020, *RAA*, 20, 163.
- Rau, A., Kulkarni, S. R., Ofek, E. O., & Yan, L. 2007, *ApJ*, 659, 1536
- Reichardt T. A., De Marco O., Iaconi R., Chamandy L., Price D. J., 2020, *MNRAS*, 494, 5333.
- Rest, A., Prieto, J. L., Walborn, N. R., et al. 2012, *Nature*, 482, 375
- Retter, A., & Marom, A. 2003, *MNRAS*, 345, L25
- Retter, A., Zhang, B., Siess, L., Levinson, A. 2006, *MNRAS*, 370, 1573.
- Ricker P. M., Taam R. E., 2012, *ApJ*, 746, 74.
- Roepke F. K., De Marco O., 2023, *Living Rev Comput Astrophys*, 9, 2
- Sand C., Ohlmann S. T., Schneider F. R. N., Pakmor R., Röpke F. K., 2020, *A&A*, 644, A60.
- Scheier, R., Hillel, S., Shiber, S., & Soker, N. 2021, *MNRAS*.
- Schreier R., Hillel S., Soker N., 2023, *MNRAS*, 520, 4182.
- Schröder S. L., MacLeod M., Loeb A., Vigna-Gómez A., Mandel I., 2020, *ApJ*, 892, 13.
- Segev, R., Sabach, E., & Soker, N. 2019, *ApJ*, 884, 58
- Shara, M. M., Moffat, A. F. J., & Webbink, R. F. 1985, *ApJ*, 294, 271
- Smith N., 2008, *ASPC*, 388, 129.
- Soker N., 2001, *MNRAS*, 325, 584.
- Soker N., 2007, *ApJ*, 661, 490.
- Soker N., 2016a, *NewA*, 47, 16.
- Soker N., 2016b, *NewAR*, 75, 1.
- Soker N., 2020, *ApJ*, 893, 20.
- Soker, N., & Gillkis, A. 2018, *MNRAS*, 475, 1198
- Soker N., Kaplan N., 2021, *RAA*, 21, 090.
- Soker N., Kashi A., 2012, *ApJ*, 746, 100.
- Soker, N., & Kashi, A. 2016, *MNRAS*, 462, 217
- Soker N., Kashi A., 2016, *MNRAS*, 462, 217.
- Soker N., Tylanda R., 2003, *ApJL*, 582, L105.
- Stritzinger M. D., Taddia F., Fraser M., Tauris T. M., Suntzeff N. B., Contreras C., Drybye S., et al., 2020a, *A&A*, 639, A103.
- Stritzinger M. D., Taddia F., Fraser M., Tauris T. M., Contreras C., Drybye S., Galbany L., et al., 2020b, *A&A*, 639, A104.
- Tylanda, R. 2005, *A&A*, 436, 1009
- Tylanda R., Górny S. K., Kamiński T., Schmidt M., 2015, *A&A*, 578, A75.
- Tylanda R., Hajduk M., Kamiński T., Udalski A., Soszyński I., Szymański M. K., Kubiak M., et al., 2011, *A&A*, 528, A114.
- Tylanda, R., Kamiński, T., Udalski, A., et al. 2013, *A&A*, 555, A16
- Tylanda R., Soker N., 2006, *A&A*, 451, 223.
- Wadhwa S. S., De Horta A., Filipović M. D., Tothill N. F. H., Arbutina B., Petrović J., Djurašević G., 2022, *RAA*, 22, 105009.
- Yalinewich, A., & Matzner, C. D. 2019, *MNRAS*, 490, 312
- Yamazaki R., Hayasaki K., Loeb A., 2017, *MNRAS*, 466, 1421.
- Zhu C.-H., Lü G.-L., Lu X.-Z., He J., 2023, *RAA*, 23, 025021.

provides fast and easy peer review for new papers in the **astro-ph** section of the arXiv, making the reviewing process simpler for authors and referees alike. Learn more at <http://astro.theoj.org>.

This paper was built using the Open Journal of Astrophysics L<sup>A</sup>T<sub>E</sub>X template. The OJA is a journal which